Hindawi
Journal of Nanomaterials
Volume 2020, Article ID 6742728, 9 pages
https://doi.org/10.1155/2020/6742728

*Research Article*

# Enhancement of Photoelectrochemical Performance of Ag@ZnO Nanowires: Experiment and Mechanism

**Yu Cai,[1] Chengbao Yao ,[1] and Jie Yuan[2]**

[1]*Key Laboratory of Photonic and Electric Bandgap Materials, Ministry of Education, School of Physics and Electronic Engineering, Harbin Normal University, Harbin, 150025 Heilongjiang, China*
[2]*Harbin Medical University, Daqing Campus, Daqing, 163319 Heilongjiang, China*

Correspondence should be addressed to Chengbao Yao; yaochengbao5@163.com

Received 5 December 2019; Revised 22 February 2020; Accepted 3 March 2020; Published 20 March 2020

Guest Editor: Edson C. da Silva Filho

Copyright © 2020 Yu Cai et al. This is an open access article distributed under the Creative Commons Attribution License, which permits unrestricted use, distribution, and reproduction in any medium, provided the original work is properly cited.

This paper focuses on the enhancement of photoelectrochemical (PEC) performance of uniform silver nanoparticles-decorated ZnO (Ag@ZnO) nanowires, which have been synthesized by two-step chemical vapor deposition to prepare ZnO nanowires then magnetron sputtering method to deposit Ag nanoparticles. Moreover, we analyzed the mechanisms of the PEC behavior of the Ag@ZnO nanowires. The PEC characteristics show that the current density of Ag@ZnO nanowires increased comparing to that of unmodified ZnO nanowires. The optimized content of the Ag-decorated ZnO photoelectrode is up to the maximum photocurrent density of 24.8 $\mu Acm^{-2}$ at 1 V vs. Ag/AgCl, which was almost four times than that of the unmodified ZnO photoelectrode. Based on the surface plasmon resonance (SPR), effect of Ag nanoparticles was enhanced PEC performance of the Ag@ZnO nanowires. Because SPR effect of Ag nanoparticles extended the light absorption and enhanced the separation efficiency of the photogenerated electron-hole pairs. The remarkable PEC properties offer metals-semiconductor compound nanostructures materials as a promising electron source for high current density applications.

## 1. Introduction

As always, zinc oxide (ZnO) materials have been studied continuously by many researchers because of its advantages of excellent characteristics and excellent features and wide range of applications [1–15]. However, to improve its electrical and optical properties, ZnO is generally doped or decorated with group various elements. Doped ZnO materials are promising candidates as conductors with high transparency in the visible light range and high conductivity [16, 17]. The conductivity, ferromagnetic, and transparency properties of doped ZnO materials have been increased in terms of present reports [18–22]. Decorated ZnO materials are promising candidates as conductors with the absorption of visible light being enhanced and the combination of photogenerated electron-holes being suppressed [23, 24]. Recently, varieties of metal-doped or decorated semiconductor compounds nanostructures morphologies [5, 25–31], such as nanowires, nanotubes, nanorods, nanoflowers, nanorings, nanobelts, nanosheets, nanowalls, nanograsses, and heterostructures, have been successfully synthesized using multiple methods, including chemical vapor deposition (CVD) [32, 33], screen printing technologies [34, 35], hydrothermal method [36, 37], hydrothermal and chemical method [38], the thermal evaporation process [39], thermal evaporation method [40], and a template-free single-step hydrothermal method [41]. However, CVD and magnetron sputtering (MS) methods are very common methods for growth of nanomaterial with different morphologies. In addition, among the various metal elements, compared to semiconductor nanoparticles, noble metal nanoparticles have considerable photostability [42–45]. The noble metal-decorated semiconductor nanomaterials increased the photon absorption rate of the photoanode and improved the photoactivity because the surface plasmon resonance (SPR) effect of metal nanoparticles induced electric field application near the oxide semiconductor surface [46]. Due to localized SPR effect, Ag nanoparticles possess strong absorptions in the visible spectrum and could improve the apparent photoactivity of the semiconductor in the visible region. There

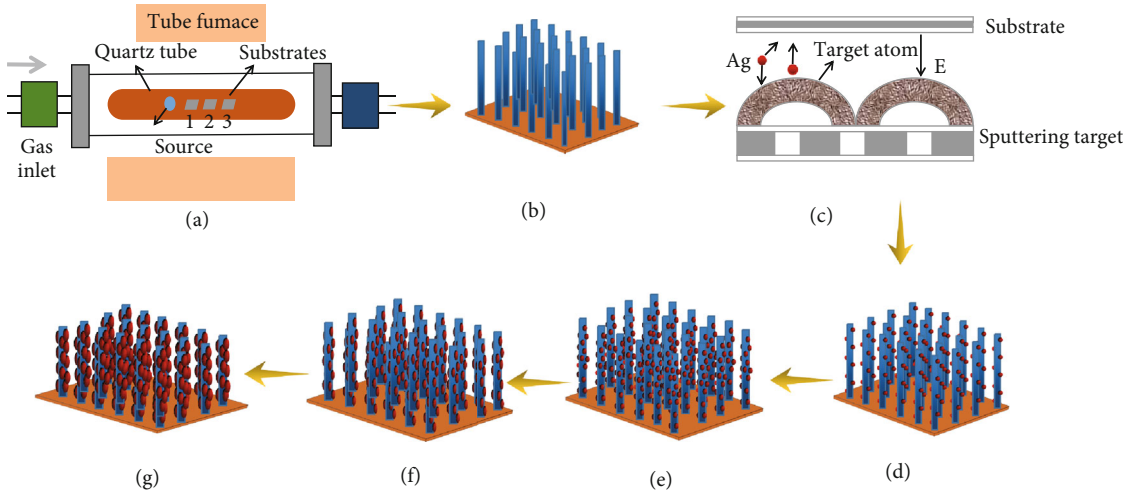


Figure 1: Growth process of Ag@ZnO NWs at the sputtering time.

are many articles reporting physical properties of silver nanoparticle-decorated ZnO with different nanostructure [47–53]. Ag nanoparticles are selected to decorate semiconductors which were widely applied in PEC devices.

In a previous report, uniform silver nanoparticles-decorated ZnO (Ag@ZnO) nanowires composite which were successfully synthesized by two-step CVD and MS method are reported [54, 55]. We studied the structure and optical properties of Ag@ZnO nanowires by magnetron sputtering method at sputtering time of 80, 100, and 120 s. However, there are no detail reports on the study of deposition parameters, which will impact on the film properties. The analysis about the PEC behavior of the Ag@ZnO nanowires is seldom reported. In the present paper, using transmission electron microscopy (TEM) and X-ray diffraction (XRD) techniques, the observed morphology and structure of Ag@ZnO nanowires were analyzed. The PEC performance of the samples was investigated. Ag@ZnO nanowires exhibit excellent PEC performance compared to unmodified ZnO nanowires, which are likely to be the potential applications in photoelectric devices.

## 2. Experimental Section

*2.1. Grown of Samples.* The Ag@ZnO nanowires were synthesized on quartz substrates by two-step CVD and MS method. The ZnO nanowires were grown by the CVD, and then Ag nanoparticles were deposited on ZnO nanowires using the MS system. As shown in Figure 1, ZnO NWs decorated with Ag nanoparticles were manufactured in the two steps of CVD and MS. The precursor is the powder of ZnO (1 g) on 1D nanostructure for nanowires. It was placed into an alumina boat and loaded into the tubular furnace. The Au-coated quartz substrates were placed downstream from the powders. The furnace was heated to a preset temperature (1250°C). Ar was used as carrier gas during growth at the constant flow rate and pressure: 100 sccm, 50 Pa for ZnO nanowires. Afterwards, the furnace was naturally cooled down to room temperature. Radio frequency target (RFT) is an Ag disc of

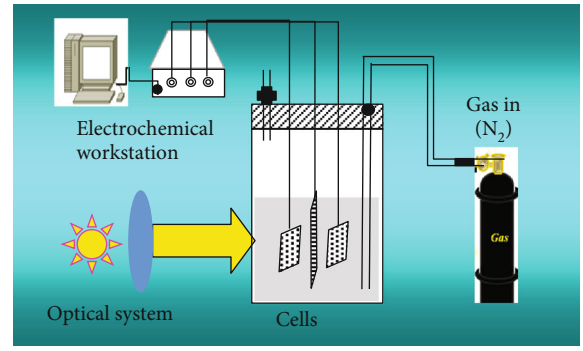


Figure 2: Schematic of the measurement of PEC for the unmodified ZnO and Ag-ZnO nanowires.

60 mm in diameter with a purity of 99.99%. The base pressure in the deposition chamber and radio frequency power were $6.0 \times 10^{-4}$ Pa and 3 W, respectively. The growth of sample proceeded in the growth ambient with the Ar of 20 sccm at a constant working pressure of 1.0 Pa, and the sputtering times are 80,100, and 120 s, respectively.

*2.2. Characteristic of Samlpes.* The morphologies and components of Ag@ZnO and unmodified ZnO nanowires were observed by using field emission scanning electron microscopy (FE-SEM), energy dispersive X-ray (EDX), and TEM. The crystallinity was analyzed by using XRD equipped with monochromated Cu Ka irradiation. PEC properties of sample photoanodes were carried out in a three-electrode cell at room temperature. Figure 2 illustrates the schematic diagram of experimental setup. Briefly, 0.05 mol/L $Na_2SO_4$ solutions were used as electrolytes, through which nitrogen was bubbled. The illumination source was a 200-W Xe arc lamp.

## 3. Results and Discussion

*3.1. The Morphologies and Structure for Ag@ZnO Nanowires.* Figures 3(a)–3(d) show the FE-SEM images of the unmodified ZnO and Ag@ZnO nanowires with different sputtering

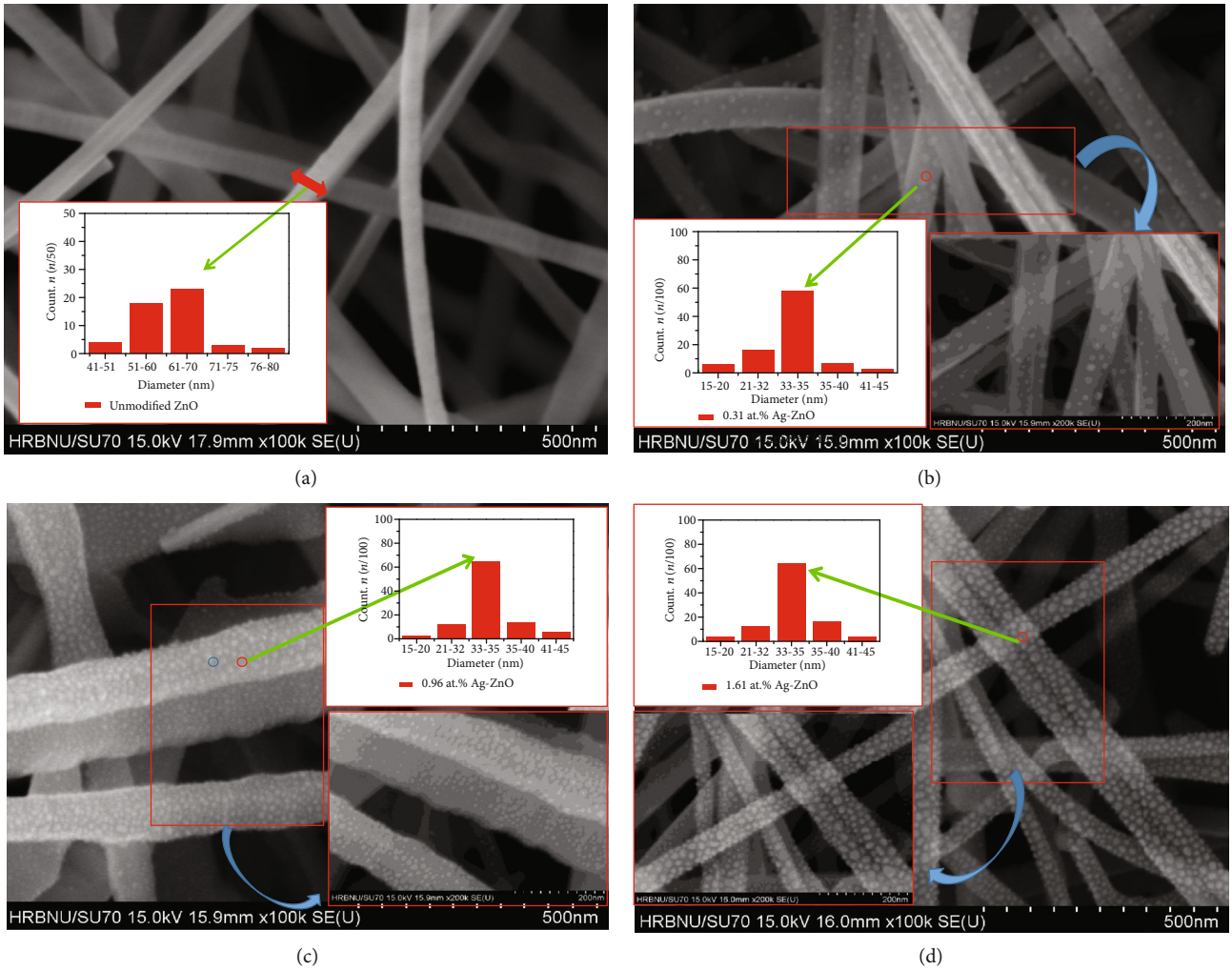


FIGURE 3: Low-magnification image FE-SEM image of (a) unmodified ZnO and (b–d) Ag@ZnO nanowires. The inset shows the distribution of the average diameter and particle size for unmodified ZnO and Ag@ZnO nanowires.

times of Ag (80,100, and 120 s), respectively. Because the average diameter and length of unmodified ZnO nanowires were approximately 65 nm and 2 $\mu$m (see the inset of Figure 3(a)), the ZnO nanowires have excellent aspect ratios. In the local magnification, Ag particles can be clearly seen, which is around 33~35 nm of most size and have a little change (see the insetof Figures 3(b)–3(d)). However, with the increase of time, Ag particle density increases and the coverage area of Ag@ZnO nanowires increases; among them, Ag particles in Figure 3(d) are the most uniform. The Ag@ZnO nanowires unfold rougher surfaces which are attributed to the adsorption of Ag nanoparticles on the surface of the ZnO nanowires.

To confirm the attachment between nanoparticles and ZnO nanowires on the surface, TEM was used, and the observed results were shown in Figures 4(a)–4(c). The figures are the TEM images of a single silver composite ZnO nanowire after ultrasonic dispersion. As can be seen from Figure 4(a), only a small number of silver nanoparticles were attached to the surface of ZnO nanowires when the sputtering time was 80 s. With the continuous increase of sputtering time of silver particles, the particle distribution density and particle size on the surface of ZnO nanowires gradually increased. When the sputtering time was 120 s, the silver particles on the surface appeared clustering. As shown in the magnification of surface particles of Ag/ZnO under high-power electron microscope, Figure 4(a) shows that the silver sputtering time was the shortest, and the crystal array of ZnO could be seen most clearly. The SAED pattern indicates that the crystal lattice of ZnO is clear and the lattice spacing is 0.28 nm, which corresponds to the diffraction crystal surface (100) of ZnO. As the sputtering time was prolonged, the number of silver particles on the surface of the nanowires increased, covering the surface of ZnO, and the crystal texture was not as clear as that in Figure 4(b). But the ZnO lattice arrangement can also be seen clearly in Figure 4(b). Moreover, in Figure 3(c), in addition to the (100) crystal plane, there is also a ZnO (110) crystal plane with lattice spacing of 0.16 nm and a silver diffraction ring.

The XRD was used to study the structure of ZnO nanowires which were modified or not with Ag. As shown in Figures 5(a)–5(d), these results indicated that the Ag@ZnO

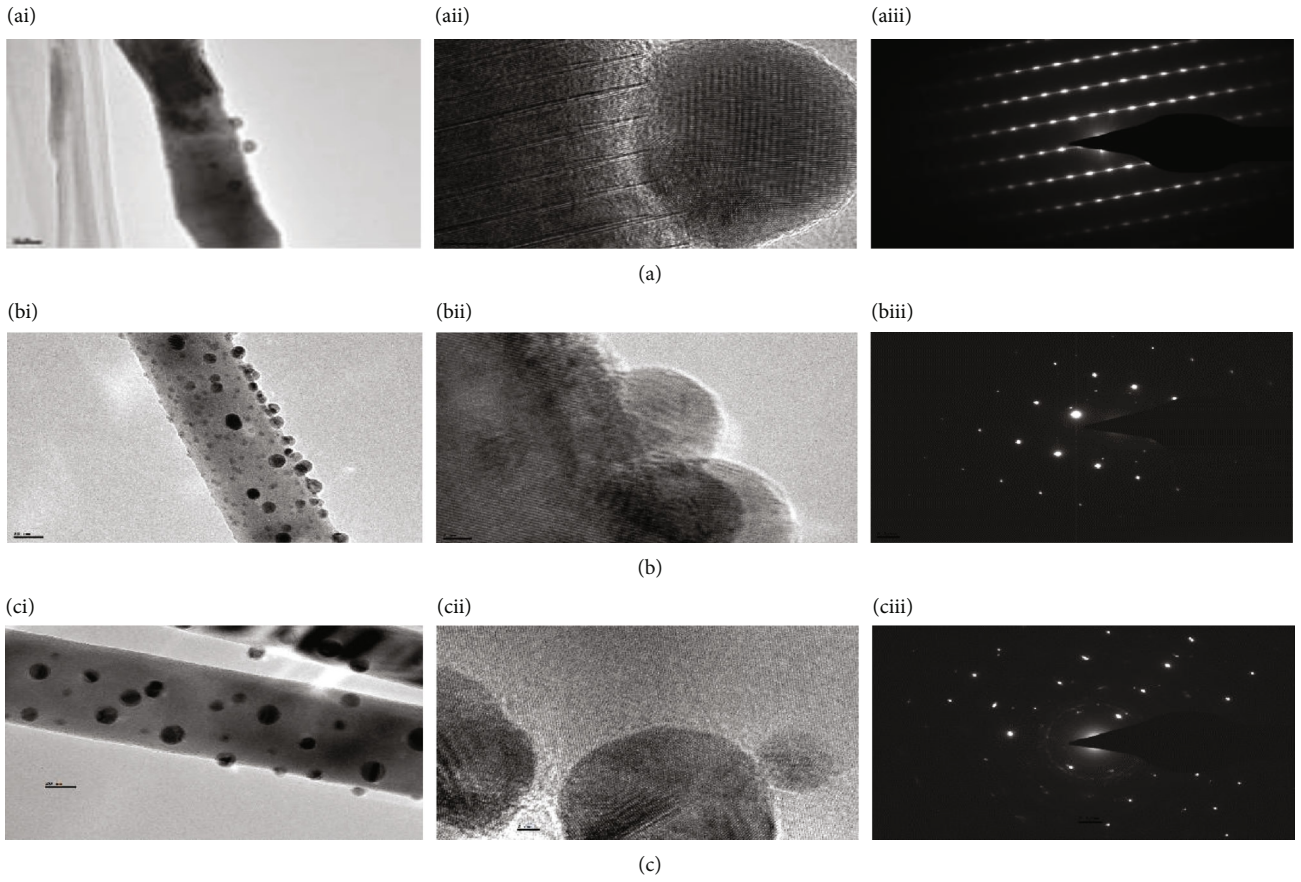


Figure 4: The TEM (ai–ci), HRTEM (aii–cii), and selected-area electron diffraction (SAED) patterns (aiii–ciii) of Ag@ZnO nanowires with sputtering times of 80, 100, and 120 s.

nanowires had high crystal crystallinity and were highly oriented to the [0002] crystal c-axis direction. The XRD results are in agreement with the TEM analysis. The observed diffraction peaks are indexed to a hexagonal wurtzite phase of ZnO, with lattice constants of $a = 0.324$ nm and $c = 0.548$ nm (JCPDS card no. 36-1451). The XRD pattern depicts a set of well-defined diffraction peaks which indicated the crystalline nature of the as-synthesized nanowires, in contrast with the other diffraction peaks, because Ag and Zn exist in the synthesized Ag@ZnO nanowires. The XRD patterns illustrated that the peaks at two theta ($2\theta$) values of 38.24° can be attributed to the prominent (111) diffraction patterns of nanocrystalline Ag particles. When the Ag content was further increased, the diffraction peak intensity of ZnO slightly decreased, while the diffraction peak intensity of Ag increased, which was due to the increase of covered surface by the Ag particles and consistent with SEM and EDX analysis. Moreover, the diffraction peaks in the XRD figure are clear and sharp, indicating that the crystallinity is good, the crystal defects are few, and no impurity peaks proves that the purity is very high.

The typical EDX results of the unmodified ZnO and Ag@ZnO nanowires were plotted in Figures 6(a)–6(d). From EDX spectra, there are clear peaks of the element (O and Zn for unmodified ZnO; O, Zn, and Ag for Ag@ZnO). The EDX data confirmed that the unmodified ZnO nanowires contained 63.61 at. % zinc and 39.39 at. % oxygen. And the Ag@ZnO nanowires contained 0.31 at. %, 0.96 at. %, and 1.61 at. % silver. The atomic percent of Ag was gradually increased with the sputtering time being longer. It is worth mentioning that with the increase of silver sputtering time, the content of zinc atoms in the sample material gradually decreases while the content of oxygen atoms gradually increases. In theory, in ZnO material, the atomic ratio of Zn and O should be 1 : 1, but intrinsic donor-type defects of the ZnO exist, namely the oxygen vacancy and zinc clearance, causing more zinc and O atoms than the theoretical value. In this experiment, sputtering time increasing of silver particles made the ratio of zinc and O atoms that were gradually adjusted from greater than 2 : 1 to approximately 1 : 1, so that it was based on silver nanoparticles composite, improved the intrinsic defects of zinc oxide.

*3.2. Photoelectrochemical Performance.* The PEC performance of unmodified ZnO and Ag@ZnO nanowires photoanodes has been studied by evaluating the current density-voltage ($J$–$V$) characteristics under light illumination. The $J$–$V$ characteristics of the sample photoanodes are shown in Figure 7. As can be seen from Figure 6(a), for the 1.0 V vs Ag/AgCI, the photocurrent density of A@ZnO nanowires reached the highest value of 24.8 $\mu$Acm$^{-2}$, which is almost six times higher than that of the unmodified ZnO photoelectrode

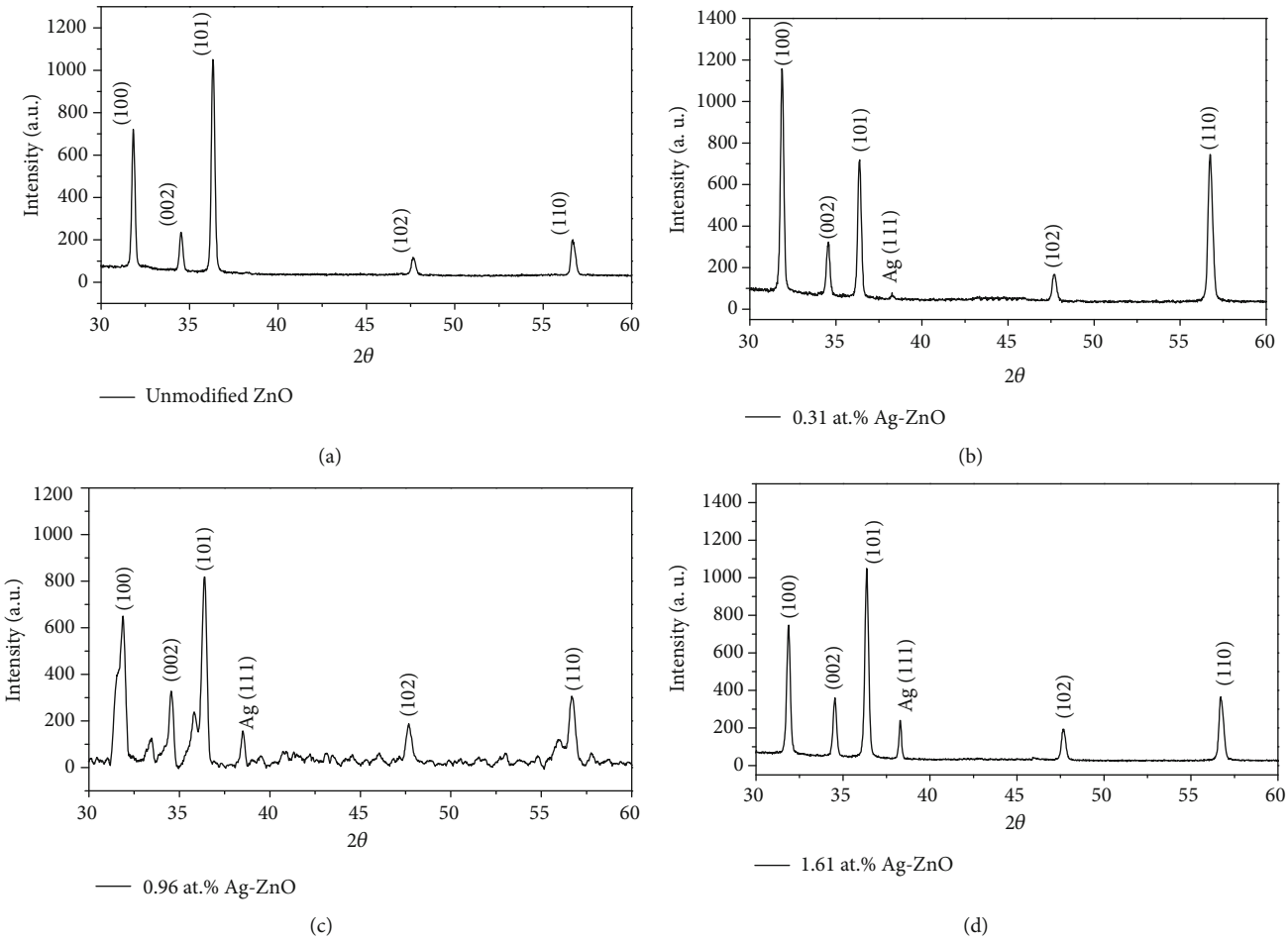


Figure 5: XRD patterns of (a) unmodified ZnO and (b–d) Ag@ZnO nanowires.

photocurrent density of 4.8 $\mu$Acm$^{-2}$. Dark scan linear sweep voltammagrams from -0.5 to +1.5 V showed a small current in the range of 0 to 40 $\mu$A/cm$^2$. When the Ag nanoparticles were modified, the SPR effect of Ag particles enhanced PEC properties. In a previous report, the charge transport within doped or decorated ZnO nanostructure is more efficient compared to ZnO nanostructured electrodes [56–59]. Figure 7(b) illustrates the instantaneous current density curves, namely *I-t* curve, visible from the figure, good light stability of the electrode to light and open to turn off the lights of the current density line, show no light-induced charge effect.

Figure 7(a) shows the photocurrent response of Ag/ZnO-coated nanowires with different silver contents. As can be seen from the Figure 7, with the increase of silver content, the photocurrent gradually increased. Among them, the optical response of 0.31 at. % Ag/ZnO is poor, the photocurrent density is very weak, and there is a certain response delay. When the silver content is 0.96 at. %, the delayed response disappears. When the silver content is 1.61 at. %, the photocurrent density increased significantly, which was about 1 mA/cm$^2$. It is proved that the increase of particle density and size on the surface of nanowires leads to better photosensitivity. As Ag particles are combined with ZnO nanowires, there is electron transfer when they contact with each other. At this time, the more Ag content there is, the more electrons it will carry. Under the action of external electric field, electrons will transfer to the opposite electrode, thus enhancing the photocurrent density.

The Ag@ZnO nanowires (for 0.96 at. % and 1.61 at. %) were selected for LSV test, and the test results are shown in Figure 7(b). At the same voltage, the current is stronger when there is more silver particles or light. The enhancement of photocurrent for Ag@ZnO nanowires was attributed to the following three factors: firstly, the local field is enhanced by SPR effect of Ag nanoparticles; secondly, the high separation efficiency of photogenic electron-hole pair; and thirdly, due to the interaction between ZnO and Ag, and reduce the charge resistance and charge compound rate. Figure 7(c) shows EIS test diagrams of Ag@ZnO nanowires with and without light. The arc radius of high silver content nanowires is smaller than that of silver content nanowires, and the arc radius with light is smaller than that without light. Since the arc radius in the figure reflects the resistance of the interface layer occurring on the electrode surface, the presence of Ag particles accelerates the electron-hole pair separation of ZnO nanowires, and the interface charge transfer is faster. The interaction between Ag and ZnO can effectively improve the separation and transfer efficiency of electron-hole pairs in ZnO and effectively inhibits the electron-hole pair

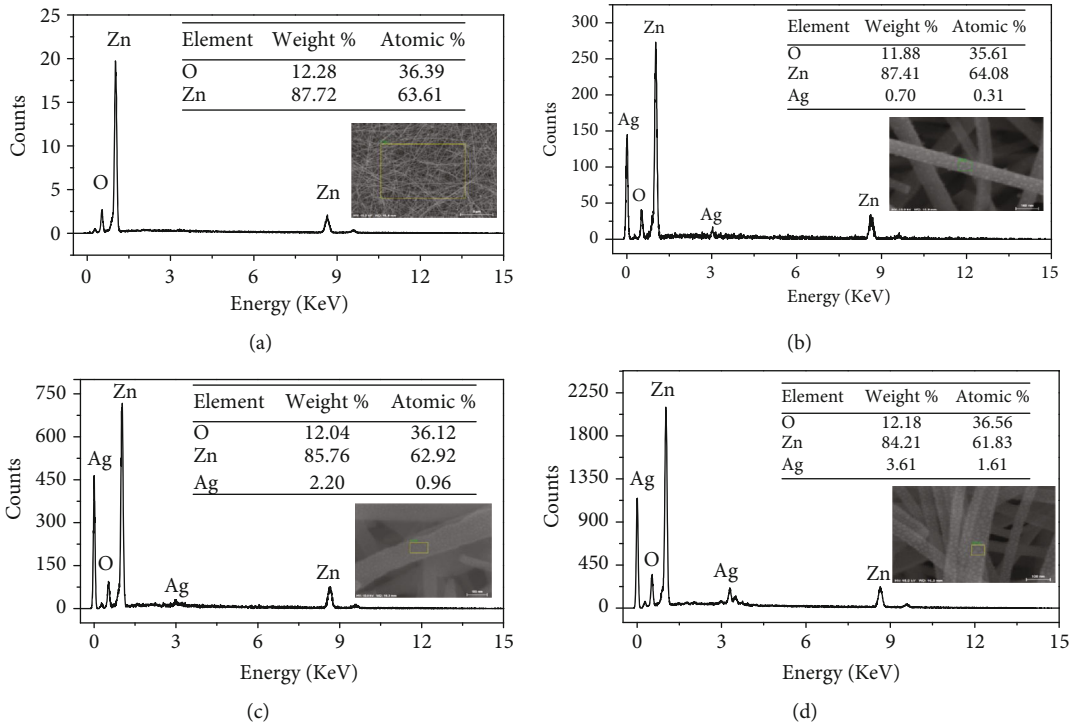


Figure 6: EDX spectra of (a) unmodified ZnO and (b–d) Ag@ZnO nanowires.

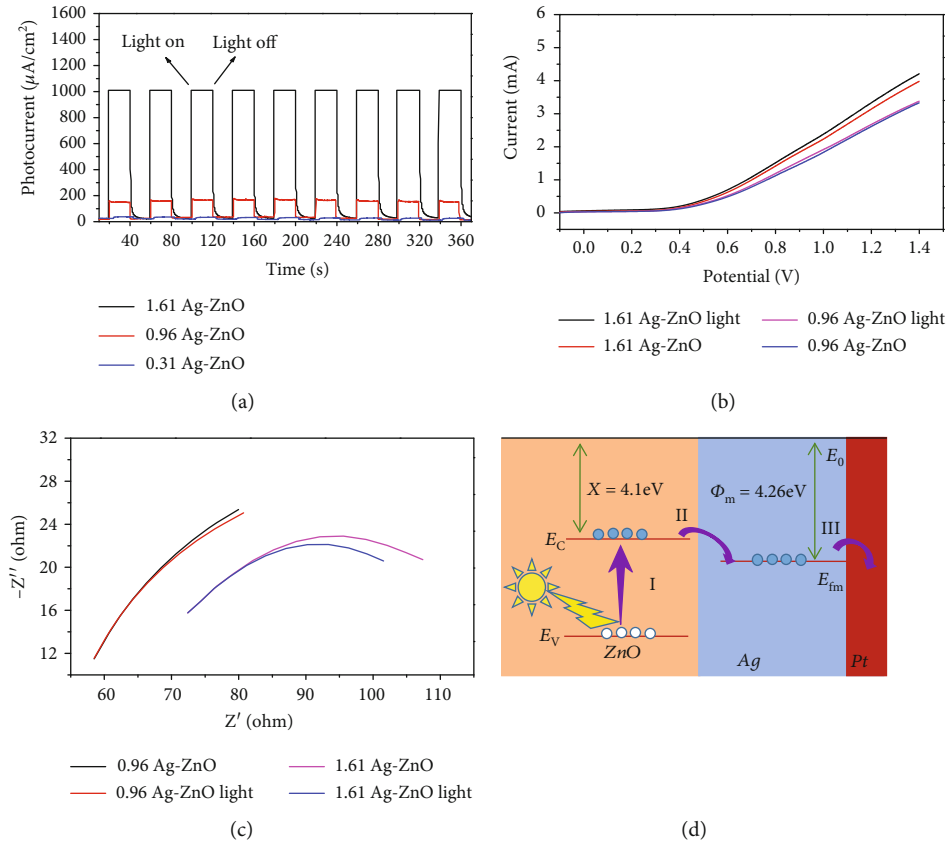


Figure 7: (a) Transient photoresponse, (b) linear sweep voltammograms, (c) EIS Nyquist plots, and (d) PEC mechanism diagram of Ag@ZnO nanowires electrodes.

recombination simultaneously. The results show that this method can effectively inhibit the electron-hole pair recombination and improve the photocatalytic activity of Ag@ZnO nanowires. We believe that Ag@ZnO nanowires can be used as effective materials to enhance photocurrent.

Based on the above discussions, the electron-transfer mechanism of the Ag@ZnO nanowires photoanode in PEC is just showed in Figure 7(d). Under the illumination, the electrons are excited to the CB of ZnO, and the same number of holes are created in the in the VB. The energy level of the bottom of the CB of ZnO is higher than the newly formed Fermi energy of the Ag@ZnO nanowires, so the photoexcited electrons would be transferred from ZnO to Ag, driven by the energy difference to enhance the separation efficiency of the photogenerated electron-hole pairs and reduces carrier recombination. Meanwhile, due to SPR excitation, Ag nanoparticles absorb the resonant photons to generate hot electrons, and hot electrons were transferred to the CB of ZnO.

## 4. Conclusions

In summary, the morphologies, structure, and PEC properties of successfully synthesized uniform Ag@ZnO nanowires by two-step CVD and MS methods were investigated. Our results indicate that the ZnO nanowires are highly crystalline with a lattice fringe of 0.28 nm, which corresponds to the (0002) planes in the ZnO crystal lattice. The average diameter of the Ag nanoparticles in the ZnO nanowires is estimated as ~34.86 nm. With the Ag nanoparticles decoration, visible emission peaks increased. Significantly, Ag@ZnO nanowires exhibit excellent PEC performance compared to unmodified ZnO nanowires. The PEC studies indicate that all electrodes are resistive in nature. The optimized content of the Ag@ZnO nanowires photoelectrode achieved the maximum photocurrent density of 24.8 $\mu Acm^{-2}$ at 1 V vs. Ag/AgCl in 0.5 M $Na_2SO_4$, which was almost four times than that of the ZnO nanowires photoelectrode under the same conditions. The enhancement of the Ag@ZnO nanowires PEC performance was attributed to the SPR effect of Ag nanoparticles, which extended the light absorption and enhanced the separation efficiency of the photogenerated electron-hole pairs. Our results indicate that Ag@ZnO nanostructures show great potential as flat panel displays, high brightness electron sources, and photoanodes in PEC devices.

## Data Availability

The data used to support the findings of this study are available from the corresponding author upon request.

## Conflicts of Interest

The authors declare that they have no conflicts of interest.

## Acknowledgments

This work was supported by the National Natural Science Foundation of China (11504072) and the University Nursing Program for Young Scholars with Creative Talents in Heilongjiang Province (No. UNPYSCT-2016179).

## References

[1] C. Klingshirn, "ZnO: material, physics and applications," *ChemPhysChem*, vol. 8, no. 6, pp. 782–803, 2007.

[2] M. Law, L. E. Greene, J. C. Johnson, R. Saykally, and P. Yang, "Nanowire dye-sensitized solar cells," *Nature Materials*, vol. 4, no. 6, pp. 455–459, 2005.

[3] D. Panda and T. Y. Tseng, "One-dimensional ZnO nanostructures: fabrication, optoelectronic properties, and device applications," *Journal of Materials Science*, vol. 48, no. 20, pp. 6849–6877, 2013.

[4] D. T. Nguyen, E. C. Shin, D. C. Cho, K. W. Chae, and J. S. Lee, "Photoelectrochemical performance of ZnO thin film anodes prepared by solution method," *International Journal of Hydrogen Energy*, vol. 39, no. 35, pp. 20764–20770, 2014.

[5] A. B. Djurišić and Y. H. Leung, "Optical properties of ZnO nanostructures," *Small*, vol. 2, no. 8-9, pp. 944–961, 2006.

[6] C. L. Hsu and S. J. Chang, "Doped ZnO 1D nanostructures: synthesis, properties, and photodetector application," *Small*, vol. 10, no. 22, pp. 4562–4585, 2014.

[7] A. B. Djurišić, A. M. C. Ng, and X. Y. Chen, "ZnO nanostructures for optoelectronics: material properties and device applications," *Progress in Quantum Electronics*, vol. 34, no. 4, pp. 191–259, 2010.

[8] J. Li, H. Fan, and X. Jia, "Multilayered ZnO nanosheets with 3D porous architectures: synthesis and gas sensing application," *The Journal of Physical Chemistry C*, vol. 114, no. 35, pp. 14684–14691, 2010.

[9] A. Baltakesmez, S. Tekmen, and S. Tüzemen, "ZnO homojunction white light-emitting diodes," *Journal of Applied Physics*, vol. 110, no. 5, 2011.

[10] M. H. Huang, S. Mao, H. Feick et al., "Room-temperature ultraviolet nanowire nanolasers," *Science*, vol. 292, no. 5523, pp. 1897–1899, 2001.

[11] C. Soci, A. Zhang, B. Xiang et al., "ZnO nanowire UV photodetectors with high internal gain," *Nano Letters*, vol. 7, no. 4, pp. 1003–1009, 2007.

[12] M. S. Arnold, P. Avouris, Z. W. Pan, and Z. L. Wang, "Field-effect transistors based on single semiconducting oxide nanobelts," *The Journal of Physical Chemistry B*, vol. 107, no. 3, pp. 659–663, 2003.

[13] X. D. Bai, P. X. Gao, Z. L. Wang, and E. G. Wang, "Dual-mode mechanical resonance of individual ZnO nanobelts," *Applied Physics Letters*, vol. 82, no. 26, pp. 4806–4808, 2003.

[14] S. Suwanboon, P. Amornpitoksuk, and A. Sukolrat, "Dependence of optical properties on doping metal, crystallite size and defect concentration of M-doped ZnO nanopowders (M = Al, Mg, Ti)," *Ceramics International*, vol. 37, no. 4, pp. 1359–1365, 2011.

[15] A. Wei, X. W. Sun, J. X. Wang et al., "Enzymatic glucose biosensor based on ZnO nanorod array grown by hydrothermal decomposition," *Applied Physics Letters*, vol. 89, no. 12, p. 123902, 2006.

[16] P.-Y. Prodhomme, A. Beya-Wakata, and G. Bester, "Nonlinear piezoelectricity in wurtzite semiconductors," *Physical Review B*, vol. 88, no. 12, p. 121304, 2013.

[17] S. J. Pearton, D. P. Norton, M. P. Ivill et al., "ZnO doped with transition metal ions," *IEEE Transactions on Electron Devices*, vol. 54, no. 5, pp. 1040–1048, 2007.

[18] G. D. Yuan, W. J. Zhang, J. S. Jie et al., "Tunable n-type conductivity and transport properties of Ga-doped ZnO nanowire arrays," *Advanced Materials*, vol. 20, no. 1, pp. 168–173, 2010.

[19] M. Y. Tan, C. B. Yao, X. Y. Yan et al., "Structural and nonlinear optical behavior of Ag-doped ZnO films," *Optical Materials*, vol. 51, pp. 133–138, 2016.

[20] C. B. Yao, K. X. Zhang, X. Wen, J. Li, Q. H. Li, and S. B. Yang, "Morphologies, field-emission and ultrafast nonlinear optical behavior of pure and Ag-doped ZnO nanostructures," *Journal of Alloys and Compounds*, vol. 698, pp. 284–290, 2017.

[21] D. Chu, Y. P. Zeng, and D. Jiang, "Synthesis of room-temperature ferromagnetic Co-doped ZnO nanocrystals under a high magnetic field," *Journal of Physical Chemistry C*, vol. 111, no. 16, pp. 5893–5897, 2007.

[22] H. B. Wang, F. Ma, Q. Q. Li et al., "Synthesis and stress relaxation of ZnO/Al-doped ZnO core-shell nanowires," *Nanoscale*, vol. 5, no. 7, pp. 2857–2863, 2013.

[23] Y. Chen, W. H. Tse, L. Chen, and J. Zhang, "Ag nanoparticles-decorated ZnO nanorod array on a mechanical flexible substrate with enhanced optical and antimicrobial properties," *Nanoscale Research Letters*, vol. 10, no. 1, article 712, 2015.

[24] S. Kalusniak, S. Sadofev, and F. Henneberger, "ZnO as a tunable metal: new types of surface plasmon polaritons," *Physical Review Letters*, vol. 112, no. 13, p. 137401, 2014.

[25] L. Schmidt-Mende and J. L. MacManus-Driscoll, "ZnO - nanostructures, defects, and devices," *Materials Today*, vol. 10, no. 5, pp. 40–48, 2007.

[26] S. Y. Li, C. Y. Lee, P. Lin, and T. Y. Tseng, "Gate-controlled ZnO nanowires for field-emission device application," *Journal of Vacuum Science & Technology B: Microelectronics and Nanometer Structures*, vol. 24, no. 1, pp. 147–151, 2006.

[27] S. M. Pimenov, V. D. Frolov, A. V. Kudryashov et al., "Electron field emission from semiconducting nanowires," *Diamond and Related Materials*, vol. 17, no. 4-5, pp. 758–763, 2008.

[28] S. S. Park, J. M. Lee, S. I. Yoon et al., "Low-temperature synthesis of one-dimensional ZnO nanostructures on screen- printed carbon nanotube films," *Physica E: Low-dimensional Systems and Nanostructures*, vol. 40, no. 7, pp. 2526–2530, 2008.

[29] S. H. Kim and D. G. Lee, "Effects of constituents in CNT pastes on the field emission characteristics of carbon nanotubes," *Journal of the Korean Institute of Electrical and Electronic Material Engineers*, vol. 24, no. 3, pp. 245–249, 2011.

[30] S. J. Kyung, J. B. Park, B. J. Park et al., "The effect of Ar neutral beam treatment of screen-printed carbon nanotubes for enhanced field emission," *Journal of Applied Physics*, vol. 101, no. 8, article 083305, 2007.

[31] N. Pan, H. Xue, M. Yu et al., "Tip-morphology-dependent field emission from ZnO nanorod arrays," *Nanotechnology*, vol. 21, no. 22, pp. 225707–225712, 2010.

[32] D. N. Montenegro, A. Souissi, C. Martínez-Tomás, V. Muñoz-Sanjosé, and V. Sallet, "Morphology transitions in ZnO nanorods grown by MOCVD," *Journal of Crystal Growth*, vol. 359, pp. 122–128, 2012.

[33] I. S. Cho, Z. Chen, A. J. Forman et al., "Branched TiO2Nanorods for photoelectrochemical hydrogen production," *Nano Letters*, vol. 11, no. 11, pp. 4978–4984, 2011.

[34] K. S. Ahn, Y. Yan, S. Shet, T. Deutsch, J. Turner, and M. Al-Jassim, "Enhanced photoelectrochemical responses of ZnO films through Ga and N codoping," *Applied Physics Letters*, vol. 91, no. 23, p. 231909, 2007.

[35] Y. Zang, X. He, J. Li et al., "Band edge emission enhancement by quadrupole surface plasmon–exciton coupling using direct-contact Ag/ZnO nanospheres," *Nanoscale*, vol. 5, no. 2, pp. 574–580, 2013.

[36] S. Gao, H. Zhang, R. Deng, X. Wang, D. Sun, and G. Zheng, "Engineering white light-emitting Eu-doped ZnO urchins by biopolymer-assisted hydrothermal method," *Applied Physics Letters*, vol. 89, no. 12, pp. 123125–123125, 2006.

[37] X. Yang, A. Wolcott, G. Wang et al., "Nitrogen-doped ZnO nanowire arrays for photoelectrochemical water splitting," *Nano Letters*, vol. 9, no. 6, pp. 2331–2336, 2009.

[38] A. S. M. Iftekhar Uddin and G. S. Chung, "Acetylene gas sensing properties of silver nanoparticles decorated ZnO morphologies with reduced graphene oxide hybrids," in *2015 IEEE SENSORS*, pp. 1–4, Busan, South Korea, November 2015.

[39] A. Umar, B. Karunagaran, E.-K. Suh, and Y. B. Hahn, "Structural and optical properties of single-crystalline ZnO nanorods grown on silicon by thermal evaporation," *Nanotechnology*, vol. 17, no. 16, pp. 4072–4077, 2006.

[40] L. M. Yu and C. C. Zhu, "Field emission characteristics study for ZnO/Ag and ZnO/CNTs composites produced by DC electrophoresis," *Applied Surface Science*, vol. 255, no. 20, pp. 8359–8362, 2009.

[41] S. S. Warule, N. S. Chaudhari, J. D. Ambekar, B. B. Kale, and M. A. More, "Hierarchical nanostructured ZnO with nanorods engendered to nanopencils and pin-cushion cactus with its field emission study," *ACS Applied Materials & Interfaces*, vol. 3, no. 9, pp. 3454–3462, 2011.

[42] J. Li, S. K. Cushing, P. Zheng et al., "Solar hydrogen generation by a CdS-Au-$TiO_2$ sandwich nanorod array enhanced with Au nanoparticle as electron relay and plasmonic photosensitizer," *American Chemical Society*, vol. 136, no. 23, pp. 8438–8449, 2014.

[43] Y. C. Pu, G. Wang, K. D. Chang et al., "Au nanostructure-decorated TiO2Nanowires exhibiting photoactivity across entire UV-visible region for photoelectrochemical water splitting," *Nano Letters*, vol. 13, no. 8, pp. 3817–3823, 2013.

[44] J. Wang, S. Pan, M. Chen, and D. A. Dixon, "Gold nanorod-enhanced light absorption and photoelectrochemical performance of $\alpha$-Fe2O3Thin-Film electrode for solar water splitting," *Journal of Physical Chemistry C*, vol. 117, no. 42, pp. 22060–22068, 2013.

[45] C. Zhang, H. Y. Xu, W. Z. Liu et al., "Enhanced ultraviolet emission from Au/Ag-nanoparticles @MgO/ZnO heterostructure light-emitting diodes: a combined effect of exciton- and photon-localized surface plasmon couplings," *Optics Express*, vol. 23, no. 12, pp. 15565–15574, 2015.

[46] X. Zhang, Y. Liu, and Z. Kang, "3D branched ZnO nanowire arrays decorated with plasmonic Au nanoparticles for high-performance photoelectrochemical water splitting," *ACS Applied Materials & Interfaces*, vol. 6, no. 6, pp. 4480–4489, 2014.

[47] Q. Tao, S. Li, C. Ma, K. Liu, and Q. Y. Zhang, "A highly sensitive and recyclable SERS substrate based on Ag-nanoparticle-decorated ZnO nanoflowers in ordered arrays," *Dalton Transactions*, vol. 44, no. 7, pp. 3447–3453, 2015.

[48] Y. H. Ko and J. S. Yu, "Silver nanoparticle decorated ZnO nanorod arrays on AZO films for light absorption

enhancement," *Physica Status Solidi A*, vol. 209, no. 2, pp. 297–301, 2012.

[49] C.-C. Yang, H.-C. Yu, Y.-K. Su, M.-Y. Chuang, C.-H. Hsiao, and T.-H. Kao, "Noise properties of Ag nanoparticle-decorated ZnO nanorod UV photodetectors," *IEEE Photonics Technology Letters*, vol. 28, no. 4, pp. 379–382, 2016.

[50] F. Li, S. Wu, L. Zhang, and Z. Li, "Ag nanoparticles decorated ZnO nanoarrays with enhanced surface-enhanced Raman scattering and field emission property," *Journal of Materials Science: Materials in Electronics*, vol. 28, no. 21, pp. 16233–16238, 2017.

[51] X. Dong, P. Yang, C. Jia, F. Yang, and D. Wang, "Ag nanoparticle-decorated ZnO nanorod arrays: synthesis, growth mechanism, and properties," *Nanoscience and Nanotechnology Letters*, vol. 6, no. 8, pp. 711–716, 2014.

[52] Q. Deng, X. Duan, D. H. L. Ng et al., "Ag nanoparticle decorated nanoporous ZnO microrods and their enhanced photocatalytic activities," *ACS Applied Materials & Interfaces*, vol. 4, no. 11, pp. 6030–6037, 2012.

[53] W. Z. Liu, H. Y. Xu, C. L. Wang et al., "Enhanced ultraviolet emission and improved spatial distribution uniformity of ZnO nanorod array light-emitting diodes via Ag nanoparticles decoration," *Nanoscale*, vol. 5, no. 18, pp. 8634–8639, 2013.

[54] K.-X. Zhang, C.-B. Yao, X. Wen, Q.-H. Li, and W.-J. Sun, "Ultrafast nonlinear optical properties and carrier dynamics of silver nanoparticle-decorated ZnO nanowires," *RSC Advances*, vol. 8, no. 46, pp. 26133–26143, 2018.

[55] K.-X. Zhang, X. Wen, C.-B. Yao et al., "Synthesis, structural and optical properties of silver nanoparticles uniformly decorated ZnO nanowires," *Chemical Physics Letters*, vol. 698, pp. 147–151, 2018.

[56] N. L. Tarwal and P. S. Patil, "Enhanced photoelectrochemical performance of Ag-ZnO thin films synthesized by spray pyrolysis technique," *Electrochimica Acta*, vol. 56, no. 18, pp. 6510–6516, 2011.

[57] K. S. Ahn, S. Shet, T. Deutsch et al., "Enhancement of photoelectrochemical response by aligned nanorods in ZnO thin films," *Journal of Power Sources*, vol. 176, no. 1, pp. 387–392, 2008.

[58] S. Shet, "Zinc oxide (ZnO) nanostructures for photoelectrochemical water splitting application," *ECS Transactions*, vol. 33, no. 38, pp. 15–25, 2011.

[59] A. Wolcott, W. A. Smith, T. R. Kuykendall, Y. Zhao, and J. Z. Zhang, "Photoelectrochemical study of nanostructured ZnO thin films for hydrogen generation from water splitting," *Advanced Functional Materials*, vol. 19, no. 12, pp. 1849–1856, 2009.